Mechanical and Microstructure Characterization of the AA6013-T4 Aluminum Alloy Welded by Laser

Eduardo Junio Menezes Carvalho[1], Milton Sérgio Fernandes de Lima[2], Bruno Nazário Coelho[3], Thiago Augusto de Sousa Moreira[1]

[1]Federal University of Western Pará, Vera Paz, Salé, 68040470, Santarém, Pará, Brazil

[2]Advanced Studies Institute, Coronel Aviador José Albano do Amarante 01 – Putim, 12228001, São José dos Campos, São Paulo, Brazil

[3]Federal University of São João del-Rei, Frei Orlando, 170, Centro, 35701970, São João del-Rei, Minas Gerais, Brazil

carvalhoejm@usp.br, miltonsflima@gmail.com, brunocoelho@ufsj.edu.br, thiago.moreira@ufopa.edu.br

Abstract. *This work aims to reveal the influence of welding parameters on the dimensional, microstructural, and mechanical characteristics of the AA6013-T4 alloy. The material was chosen due to its excellent properties and for being widely utilized in the aerospace industry. The variable process parameters employed were laser power of 1200 and 1400 W; and welding speed of 0.08 and 0.1 m/s. The joints were butt welded, without metal addition, and in single pass by a high power Yb:fiber laser. Optical microscopy and tensile testing were used to characterize the welded samples. Results revealed that the variation of the process parameters modified the weld beads geometry. The weld microstructure is composed of columnar dendrites at the edge and equiaxial at the center. Zones of liquation occurred next to the melting lines, propitiating the formation of micropores and microcracks. Due to the low solidification rate, the weldment achieved using a laser power of 1200 W and speed of 0.08 m/s gave a better performance in the tensile testing, with the maximum stress, yield stress and deformation reaching 69%, 84% and 22%, respectively, of the base material. However, the best process stability was observed when a laser power of 1200 W and speed of 0.1 m/s were employed.*

Resumo. *Este trabalho tem como objetivo revelar a influência dos parâmetros de soldagem nas características dimensionais, microestruturais e mecânicas da liga AA6013-T4. O material foi escolhido devido às suas excelentes propriedades e por ser amplamente utilizado na indústria aeroespacial. Os parâmetros variáveis de processo empregados foram potência do laser de 1200 e 1400 W; e velocidade de soldagem de 0,08 e 0,1 m / s. As juntas foram soldadas a topo, sem adição de metal, e em uma única passagem por um laser Yb: fibra de alta potência. Microscopia óptica e ensaios de tração foram utilizados para caracterizar as amostras soldadas. Os resultados revelaram que a variação dos parâmetros de processo modificou a geometria dos cordões de solda. A microestrutura da solda é composta por dendritas colunares na borda e equiaxial no centro. Zonas de liquação ocorreram próximas às linhas de fusão, propiciando a formação de microporos e microfissuras. Devido à baixa taxa de solidificação, a soldagem obtida com uma potência de laser de 1200 W e velocidade de 0,08 m / s, proporcionou um melhor desempenho nos teste de tração, com máxima tensão, tensão de escoamento e deformação*

alcançando 69%, 84% e 22%, respectivamente, do material base. No entanto, a melhor estabilidade de processo foi observada quando a potência de laser de 1200 W e velocidade de 0,1 m / s foram empregadas.

1. Introduction

The aerospace industry is constantly searching for methods to reduce weight and cost of aircraft, leading to the development of new technologies capable of overcoming the riveting process. Materials with a good ratio between mechanical strength and density, such as aluminum alloys, started to replace the traditionally applied steel [1]. Therefore, through the advance of technology and metallic alloys enrichment, it was possible to enhance the solidification crack formation resistance, making the welding an option for the joining of aerospace structures [2].

The first laser entered the scientific life in 1960 and, since then, several types of researches have been carried out. Due to its progress, this tool is among the most advanced materials processing methods, occupying a prominent position in the industry [3]. The fiber laser, which emerged as one of the most powerful laser systems of the twentieth century [4], brought with it attributes that make it ideal for welding and cutting metal [5]. Furthermore, its characteristics allow excellent penetration, which is essential to produce welding in highly reflective metals, as is the case of aluminum [6].

There are apparent advantages to the partial replacement of riveting by the welding. However, stringent quality control criteria induced manufacturers to invest in new technologies [7]. In this scenario came the laser welding, which proved to be promising for the aerospace sector when producing welds with low thermal input and high aspect ratio [8]. Also, it allows the reduction of weight and manufacturing time, and elimination of holes which makes the structure less susceptible to corrosion [9].

Scientific studies that approach the process parameters are essentials to comprehend the characteristics that can be achieved and thus make the application of laser welding in the aeronautical vehicle structure more secure. Therefore, this work sought to analyze the influence of laser welding parameters on the dimensional, microstructural, and mechanical characteristics of AA6013-T4 joints.

Equations (1), (2), and (3) are applied to calculate power density, interaction time, and specific energy point, respectively.

$$Power\ density = \frac{Laser\ Power}{Area_{beam}} \quad (1)$$

$$Interaction\ time = \frac{Diameter_{beam}}{Welding\ speed} \quad (2)$$

$$Specific\ point\ energy = Power\ density \times interaction\ time \times Area_{beam} \quad (3)$$

2. Materials and Methods

Materials. Due to its excellent properties and for being widely utilized in the aeronautical industry, the chosen material of study was the AA6013-T4 aluminum alloy. Tables 1 and 2 show the mechanical properties and chemical composition of the material.

Table 1: AA6013-T4 mechanical properties [10].

Properties	AA 6013-T4
Tensile strength (MPa)	325
Yield strength (MPa)	185
Deformation (%)	24

Table 2: AA6013 chemical composition, in weight percentage [10].

Element	Si	Fe	Cu	Mn	Mg	Cr	Zn	Ti
Minimum	0.60	-	0.60	0.20	0.80	-	-	-
Maximum	1.00	0.50	1.10	0.80	1.20	0.10	0.25	0.10

Workstation. The experiment was carried out in the Multiuser Development Laboratory and Lasers and Optics Applications (Dedalo) of the Institute of Advanced Studies (IEAv/ITA). The present laser is an IPG Photonics, model YLR-2000, with an output power up to 2.0 kW and wavelength of 1.08 µm. A coupling unit made the connection between the output fiber (50 µm in diameter and 5.0 m in length) and the secondary fiber (100 µm in diameter and 10 m in length), which was interconnected to an optical collimator to form the beam coupling system. The focal length of 160 mm projected a beam with 0.1 mm diameter on the surface of the material.

The station was also equipped with two auxiliary gas systems, nitrogen as the process gas and helium as the protection gas. The first was used to prevent optic damage, and the second was applied to create an atmosphere to avoid undesired reactions as oxidation and low laser absorption at the material's surface. Figure 1 illustrates the workstation.

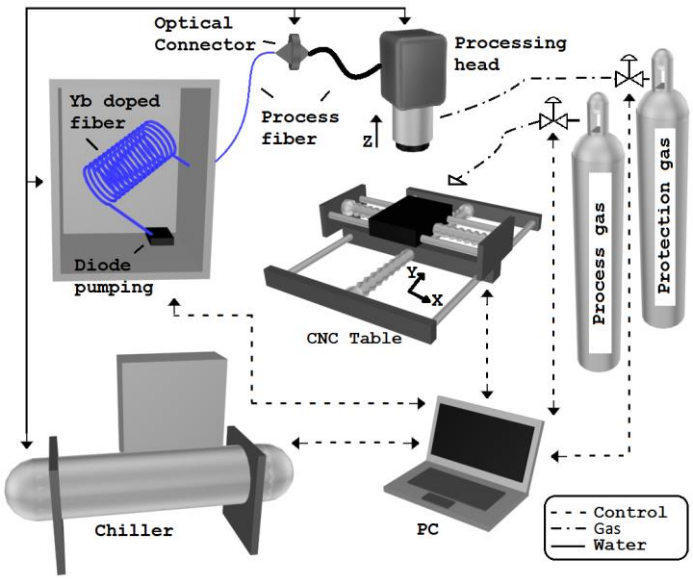

Figure 1: Materials processing station with Yb:fiber laser [11].

Welding Methodology. The laser welding process has a wide range of variables that significantly influences the material's characteristics. Therefore, it is suggested to choose a limited number of parameters to characterize its effects adequately. For materials with high reflectivity, as in the present case, it is advised to adjust the sample in five degrees to avoid reflection effect at the optic's cavity, so that won't cause any damage to the laser's cavity [12]. Furthermore, the laser beam cannot be at 90° of the material's surface due to potency loss and laser deterioration caused by reflection properties [13].

The aluminum plates were butt welded, without metal addition and in a single pass by the keyhole method. The parameters characterized were laser power and welding speed. The beam was adjusted to five degrees perpendicular to the welding direction to avoid potency loss and laser deterioration. Table 3 and Table 4 present the variables and constants, respectively.

Table 3: Welding process parameters under evaluation.

Test specimen	System parameters		Fundamental material interaction parameters		
	Power, P [kW]	Welding speed, WS [m/s]	Power Density, PD [kW/m^2]	Interaction time, T_i [s]	Specific point energy, E_{sp} [J]
P1	1.2	0.1	1.53E+8	0.00100	1.2
P2	1.2	0.08	1.53E+8	0.00125	1.5
P3	1.4	0.1	1.78E+8	0.00100	1.4

Table 4: Welding process parameters under no evaluation.

Laser beam focus	Focal distance [m]	Beam diameter [m]	Protection gas [l/s]	Beam inclination angle [°]
Surface	0.16	0.0001	0.33	5

Test Specimens Preparation and Analysis. The presence of contaminating agents on the material's surface can extremely affect the weld bead quality. Therefore, it is essential to prepare the aluminum plate surfaces adequately. After the welding process, the plates were cut using a guillotine, resulting in eighteen test specimens for the tensile test (Figure 2.a) and three for the microstructural analysis (Figure 2.b). The incidence of defects in the plate edges, commonly present in laser welding, make them discardable, to avoid incorrect interpretation of data.

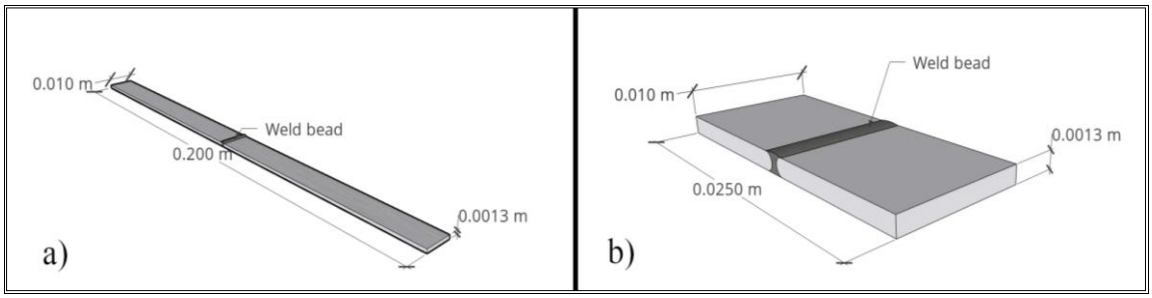

Figure 2: (a) Tensile testing and (b) microstructural analysis test specimens.

The microstructural analysis specimens were mounted in Bakelite, treated with sandpaper (100# to 1200#), polished with alumina and diamond paste (1.0 and 0.25 µm), and treated with Keller reagent (2.0 ml of HF, 3.0 ml of HCl, 5.0 ml of HNO_3 and 190 ml of H_2O) for 20 seconds. After the chemical attack, the specimens were cleaned with water and compressed air jet. The *Axio Imager.A2m Zeiss* microscope acquired the images, and the *Image J software* evaluated its dimensional characteristics. Furthermore, an *Emic 23-300* universal testing machine was set to carry on the tensile testing, and a comparison was made between the base material and the processed one, by mean and standard variation statistical analysis, was able to distinguish their features. The tensile testing was conducted according with ASTM E8/E8M standard [14].

3. Results and Discussion

Dimensional and Microstructure Characteristics. The weld beads width increases in size according to the power increase and welding speed decrease. Figure 3 shows the cross sections of the weld beads, and Table 5 summarizes its measurements.

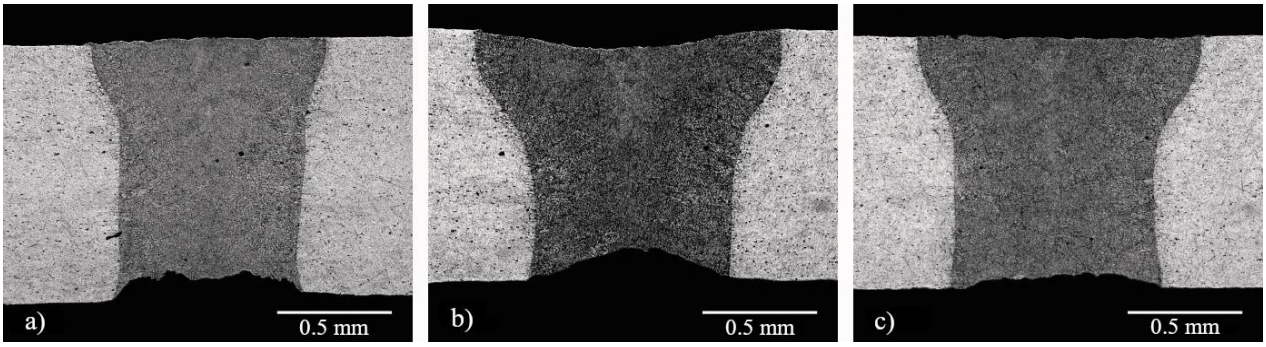

Figure 3: Weld bead cross section of a) P1, b) P2 and c) P3.

Table 5: Thickness and width measures of the weld beads.

Test specimen	Thickness[m]	Width [m]			
		Top	Mid	Base	Mean
P1	1.17E-03	1.02E-03	8.08E-04	8.11E-04	8.80E-04
P2	9.74E-04	1.34E-03	9.06E-04	8.72E-04	1.04E-03
P3	1.15E-03	1.23E-03	8.81E-04	9.23E-04	1.01E-03

Extensively studies on the laser welding control parameters have been carried out. Suder [15], for example, defined the process by power density, interaction time, and specific energy point. Also, the interaction time controls the weld bead width. Reijonen [16] showed that the laser power increase, for a constant interaction time, causes a growth in the weld width. Siqueira [5] and Carvalho [17] found that the average weld bead width increases in size with laser power increase and welding speed decrease.

Excess of interaction time causes distortions on the surface and root of the weld bead, probably due to eruptions, spattering, and rejection of material [18]. The increment of power promotes the elongation of the melted zone (MZ) and the elevation of temperature, favoring the production of defects such as porosity [11]. These events contribute to the weld bead thickness decrease.

Similar to Higashi [9], the microstructure near the melting lines (Figure 4), where the solidification is slower, was composed of columnar dendrites oriented towards the center of the weld bead. In the region where the cooling rate is highest, that is, at the center of the weld bead (Figure 5), the microstructure was formed by indefinitely oriented equiaxed dendrites. According to Oliveira [18], such characteristic tends to reduce the susceptibility to cracks by uniformly distributing the solidification stresses in the grain boundaries.

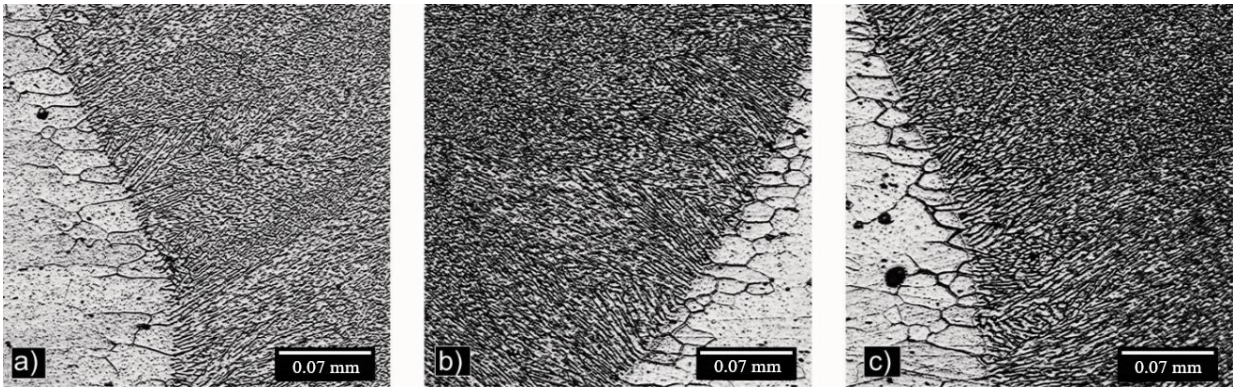

Figure 4: Fusion line microstructure of a) P1, b) P2 and c) P3.

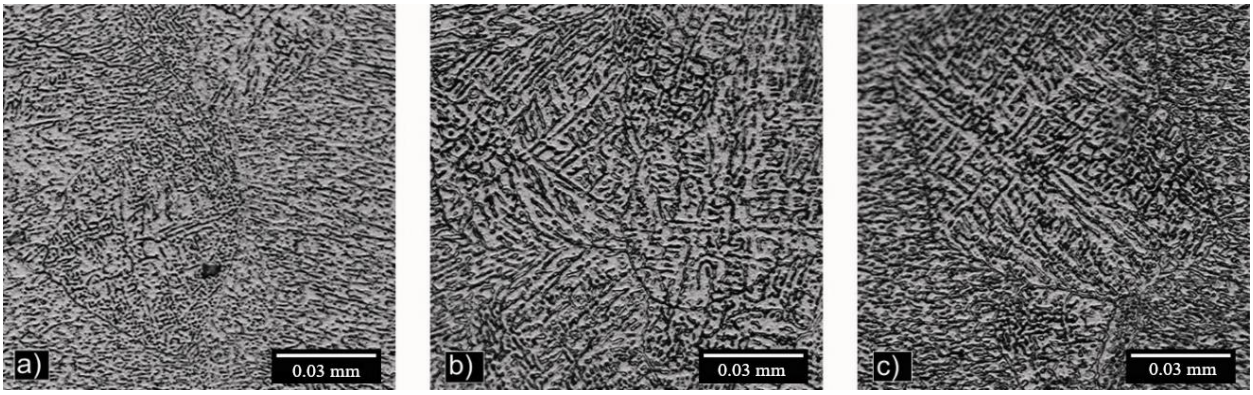

Figure 5: Center microstructure of a) P1, b) P2 and c) P3.

Figure 4 shows darker contours, called liquation zones, at the interface between the melted zone (MZ) and the thermally affected zone (TAZ). Siqueira [5] explains that this phenomenon happens due to the fusion of the adjacent grain contours, which can result in liquation cracking if they do not support the solidification stresses.

Oliveira [18] observed the same event and suggested that heat treatment could minimize it. However, Siqueira [10] subjected the AA6013 alloy to heat treatments of 190º C for 4 hours and 205° C for 2 hours and concluded that both, zones of liquation and hot cracks, were not altered.

At the interface between MZ and TAZ, the formation of micropores is observed, indicating that there were dissolved gases in the melted pool, usually hydrogen or shielding gas. The porosity is associated with several factors, mainly type and flux of shielding gas, welding speed, power, focusing conditions, sample surface preparation, and keyhole instability [19]. Figures 6 and 7 illustrate the found defects.

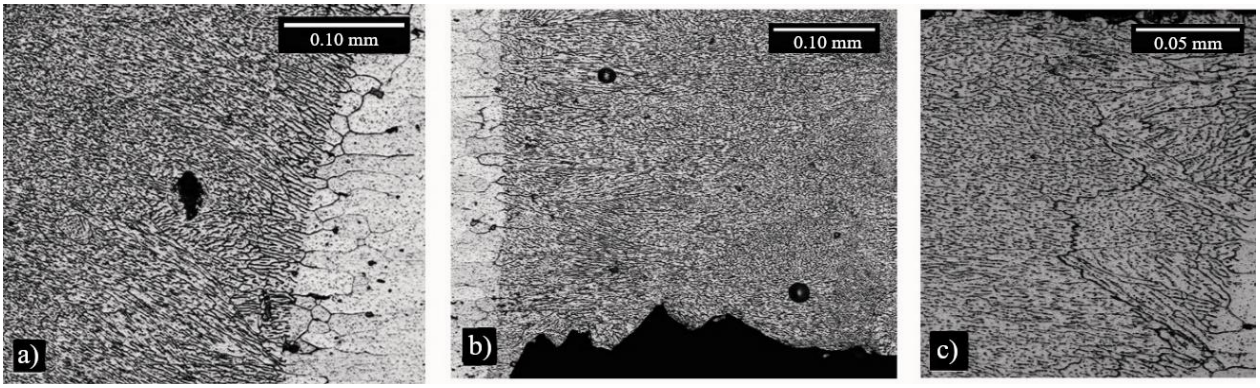

Figure 6: (a) and (b) show porosity and (c) microcracks on P1.

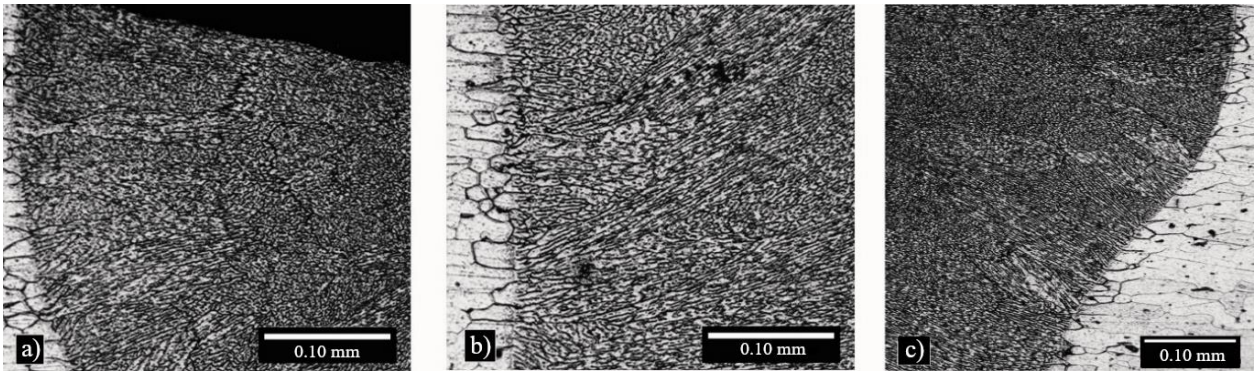

Figure 7: (a) and (b) show microcracks on P2 and (c) on P3.

Analogous to Piorino [20], laser welding provided the formation of solidification microcracks, which start in the liquation zone and propagate through the weld bead through the grain boundaries. This type of defect is associated with film formation of liquid material segregated between the grain boundaries and the inability of this structure to withstand the stresses resulting from the solidification. It generally occurs in the center of the weld bead, but it is possible to happen in different locations and orientations [19; 21].

Siqueira [19] concluded that it is possible to reduce the formation of cracks in the AA6013-T4 alloy by only increasing the interaction time of the welding energy.

Mechanical Characteristics. The dispersion present in the tensile test proves that the parameters used generated instabilities and, consequently, defects. Figure 8 presents the ultimate tensile strength and standard deviation of the AA6013-T4 alloy.

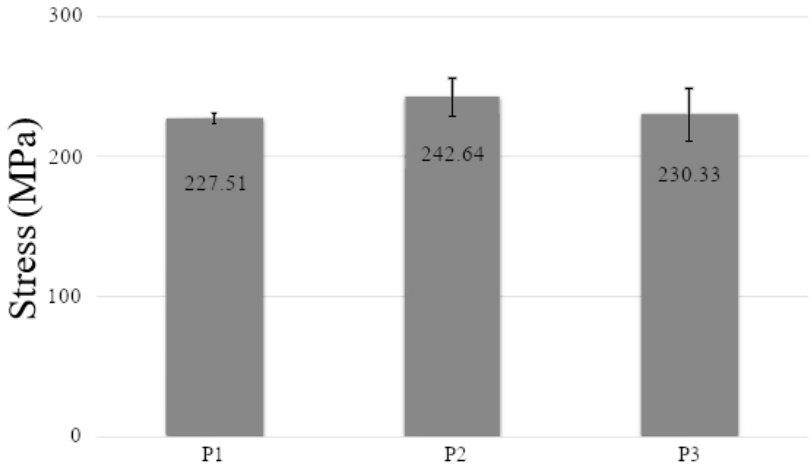

Figure 8: Maximum tensile strength and standard deviation of the AA6013-T4 alloy.

The process parameter P1 showed a dispersion approximately three times smaller than P2, and almost five times smaller than P3, indicating defects by keyhole instability. Concerning ultimate tensile strength, yield strength, and deformation, the specimen P2 reached 69%, 84%, and 22%, respectively, of the base material. Table 6 summarizes these values.

Table 6: Tensile testing mean value.

Test Specimen	P1	P2	P3	BM [10]
Ultimate tensile strength (MPa)	227.51	242.64	230.33	325
Yield strength (MPa)	184.62	194.05	187.90	185
deformation (%)	5.89	6.04	4.80	24

According to Holzer et al. [21], the tensile strength of the base material (BM) cannot be achieved because of three reasons: the heat distribution causes MZ and TAZ to soften, the loss of volume and the formation of splashes decrease the cross-sectional area and the solidification cracks occur and also reduce the strength.

4. Conclusions

Both parameters varied in the experiment modify the geometry of the weld bead. Its width increases in size with laser power increase and welding speed decrease, and even in cases where the beam diameter is kept constant, the width increases as the specific energy point intensifies.

The microstructure, similar for all conditions, is composed of columnar dendrites at the edge of the bead, where the solidification is slower, and equiaxial dendrites at its center, region with high cooling rate.

The process promoted the development of liquation zones near the melting lines, causing the formation of micropores and microcracks.

The lower solidification rate assured to P2 mechanical properties close to that of the base material (MB). However, P1 demonstrated higher stability due to the lower thermal input applied.

Acknowledgments

The authors thank the Institute of Advanced Studies (IEAv / ITA) for the infrastructure to carry out the work and the Federal University of Western Pará (UFOPA) for granting the experience on the Program of External Academic Mobility.

References

[1] T.A.S. Moreira, Caracterização microestrutural e textural, por difração de elétrons retroespalhados (EBSD), da liga de alumínio AA5052 soldada a laser, Tese M.Sc, UFOP, Ouro Preto, MG, Brasil, 2014.

[2] D.F.V. Mattos, Estudo da propagação de trinca em AA 6013-T4 soldado com laser de Yb: fibra de alta potência, Tese M.Sc, ITA, São José dos Campos, SP, Brasil, 2013.

[3] A.C. Oliveira, Microssoldagem em chapas finas utilizando um laser de Cu-Hbr, Tese M.Sc, ITA, São José dos Campos, SP, Brasil, 2006.

[4] M. Reiter, Partial penetration fiber laser welding on austenitic stainless steel, Tese de M.Sc, OSU, Columbus, OH, Estados Unidos, 2009.

[5] G.R. Siqueira, Soldagem a laser autógena da liga de alumínio aeronáutico AA6013, Tese de M.Sc, ITA, São José dos Campos, SP, Brasil, 2007.

[6] A.G. Paleocrassas, Process characterization of low speed, fiber laser welding of AA 7075-T6 application to fatigue crack repair, Tese de D.Sc, NSCU, Raleigh, NC, Estados Unidos, 2009.

[7] E.J.F. Soares, Tratamento superficial a laser dos aços AISI 1045 e AISI 4340, Tese de D.Sc, Unicamp, Campinas, SP, Brasil, 2005.

[8] L.V. Silva, Estudos dos mecanismos envolvidos em processos de endurecimento superficial a laser de ligas a base de alumínio, Tese de M.Sc, USP, São Paulo, SP, Brasil, 2011.

[9] A.L.C. Higashi, Soldagem de uma liga de alumínio-cobre-lítio utilizando laser a fibra, Tese M.Sc, ITA, São José dos Campos, SP, Brasil, 2011.

[10] R.H.M. Siqueira, Caracterização mecânica e microestrutural de juntas de alumínio 6013 T4 soldados a laser, Tese de M.Sc, Unesp, Guaratinguetá, SP, Brasil, 2012.

[11] B.N. Coelho, Soldagem do aço inoxidável AISI 316 com laser a fibra de alta potência, Revista Matéria, v. 18, n. 03, 2013.

[12] W.M. Steen, Laser Material Processing. [S.1.]: Springer-Verlag. ISBN 3-540-19670-6.

[13] B.N. Coelho, Soldagem a laser dos aços inoxidáveis AISI 304 e AISI 316: Análise microestrutural em função dos parâmetros operacionais, Tese M.Sc, UFOP, Ouro Preto, MG, Brasil, 2012.

[14] ASTM: American Society for Testing and Materials. ASTM E8/E8M. Standard Test Methods for Tension Testing of Metallic Materials (2013).

[15] W.J. Suder, Investigation of the effects of basic laser material interaction parameters in laser welding, Journal of Laser Applications, vol. 24, n. 3, 2012.

[16] J. Reijonen, The effect of focal point parameters in fiber laser Welding of structural steel. LUT, Graduation thesis, Lappeenranta, Carélia do Sul, Finlândia, 2015.

[17] S.M. Carvalho, Soldagem com laser a fibra do aço 300M de alta resistência, Tese M.Sc, ITA, São José dos Campos, SP, Brasil, 2009.

[18] A.C. Oliveira, Soldagem de alumínio estrutural aeronáutico utilizando laser a fibra de alta potência. Tese D.Sc, ITA, São José dos Campos, SP, Brasil, 2011.

[19] R.H.M. Siqueira, Soldagem a laser autógena em passe único de juntas de alumínio AA 6013-T4 com alta resistência mecânica, Tese D.Sc, ITA, São José dos Campos, SP, Brasil, 2016.

[20] N.M. Piorino, Caracterização mecânica e microestrutural de soldas a laser em alumínio aeronáutico, Trabalho de conclusão de curso, Univap, São José dos Campos, SP, 2011.

[21] M. Holzer, Change of hot cracking susceptibility in Welding of high strength Aluminum alloy AA 7075, Physics Procedia, Elsevier Science, v. 83, pp. 463 – 471, 2016.